15. TRANSITION FIXING FOR HYPERSONIC FLOW

By James R. Sterrett, E. Leon Morrisette, Allen H. Whitehead, Jr.
Langley Research Center

and

Raymond M. Hicks
Ames Research Center

SUMMARY

Present wind-tunnel facilities lack the capability to duplicate the Reynolds number associated with the hypersonic-cruise vehicle. As a means of overcoming this problem, attention is being given to artificial promotion of transition by means of surface roughness. At lower speeds, boundary-layer roughness has been used successfully. However, at hypersonic speeds, the required roughness height is so large that the method raises many questions. This paper considers these questions and examines the overall problems associated with boundary-layer "trips" to produce turbulence at hypersonic conditions.

The data indicate that the required roughness heights are so large that whether trips should be used in hypersonic wind-tunnel tests depends upon the particular purpose of any experiment. For example, an engineer can successfully use trips to study the heat transfer associated with an aircraft component or to produce turbulent flow in front of an inlet or control that otherwise might be transitional or laminar. However, at the present time, trips cannot be used when an accurate value of the total drag of a configuration is required because of the large pressure drag associated with the roughness elements. With additional study, the drag associated with the roughness elements could probably be determined accurately. The vortex shedding that occurs in the lee side of delta wings at moderate angles of attack places further limitations on the use of trips for wind-tunnel simulations of hypersonic cruise vehicles. For any test, care must be taken to dimension the trips properly.

15

INTRODUCTION

Turbulent flow is known to exist over most aircraft configurations at hypersonic speeds, yet laminar flow exists over large parts of wind-tunnel models at these speeds. In order to provide proper simulation in the hypersonic range, methods of producing turbulent flow near the leading edge of wind-tunnel models are being studied. At lower speeds, boundary-layer roughness elements have been used successfully (for example, in ref. 1); however, the required roughness height is small as compared with the boundary-layer thickness. At hypersonic Mach numbers, the roughness elements (trips) must be approximately as high as the boundary layer before even the position of transition is

affected. Small trips can even delay transition. (See ref. 2.) Since the roughness heights required to promote transition at hypersonic speeds are so large, the method raises many questions, such as: "Does a tripped turbulent boundary layer behave in the same way as a natural trubulent boundary layer?" and "How large is the drag associated with the tripping element?" In this presentation these questions and the overall problems associated with boundary-layer trips at hypersonic conditions are discussed.

SYMBOLS

C_D	coefficient of drag, $\frac{\text{Drag}}{q_\infty S}$
ΔC_D	increase in coefficient of drag due to pressure drag of roughness elements
C_F	skin-friction coefficient
c	chord (see fig. 12)
d	diameter of roughness elements
k	vertical height of roughness above plate
L	length of configuration
M	Mach number
N_{St}	Stanton number
p	static pressure
q_∞	free-stream dynamic pressure
R_k	Reynolds number based on fluid conditions at top of roughness elements and height of roughness, $\frac{\rho_k u_k k}{\mu_k}$
$R_{k,c}$	Reynolds number based on fluid conditions at top of roughness necessary to move turbulent flow close to trip position
R_L	Reynolds number based on model length
$R_{x,k}$	Reynolds number based on conditions at outer edge of boundary layer and distance from leading edge to roughness position, $\frac{\rho_o u_o x_k}{\mu_o}$

$R_{x,tr}$ Reynolds number based on conditions at outer edge of boundary layer and position where boundary layer becomes turbulent, $\frac{\rho_o u_o x_t}{\mu_o}$ (see fig. 2)

R_v Reynolds number based on distance from virtual origin, $\frac{\rho_o u_o (x - x_v)}{\mu_o}$

R_∞ free-stream Reynolds number

S planform area of configuration

s lateral spacing of center of roughness elements

u velocity component of flow parallel to surface

t average diameter (thickness) of leading edge

x distance from leading edge or distance from junction of delta wing and flap

x_k distance from leading edge to roughness position

x_t distance from leading edge to position where flow becomes turbulent

y vertical distance measured from plate surface

α angle of attack

δ boundary-layer thickness based on velocity

δ_f flap angle (see fig. 10)

δ_k boundary-layer thickness on smooth model at roughness position

δ^* boundary-layer displacement thickness

ρ density

μ viscosity

Subscripts:

l local

k conditions at top of roughness

o local conditions at outer edge of boundary layer

∞ free stream

v virtual origin

DISCUSSION

Previous work on boundary-layer transition has indicated that the process by which trips (roughness) produce turbulent flow is for the trips to produce some type of vortex flow downstream of a tripping element. An example of this phenomenon is shown in figure 1. The lower part of the figure shows paint patterns taken downstream of a sphere and reported in reference 3. The sphere was one of many which were placed on a blunted cone as is illustrated in the top part of figure 1. This figure shows that at least two vortices are produced by each roughness sphere. Similar results were reported in references 4 and 5. The effects of these vortices are shown as dark patterns, where the flow scrubs the surface and produces a high temperature. Vortices dissipate and form turbulent flow very similar to wake flows. (See, for example, refs. 6 and 7.) How soon they form turbulent flow depends very strongly upon the local Reynolds number. In fact, if the Reynolds number associated with the trip is too low, these vortices will not be produced. (See ref. 7.) On the other hand, if the roughness sphere is too large, spanwise disturbances resulting from these vortices will persist very far downstream, as is shown in reference 3.

Two methods often used to determine when turbulent flow exists are illustrated in figure 2. One method is to examine velocity profiles obtained with a pressure probe. This method is very tedious to use and the probe apparently causes distortions in the boundary layer near the surface. Examples of this latter effect are seen by comparing the data shown for both natural and tripped conditions. To compare several profiles and to determine where transition occurred is difficult because of these probe distortions. However, the method of using the location of the maximum pressure from a total-pressure tube traversed longitudinally along the model surface to locate the beginning of turbulent flow, as illustrated in reference 8, has been used successfully. The method generally used to detect transition in the present investigation is by heat-transfer measurements. An example is shown on the left-hand side of figure 2 where the heat-transfer rate in terms of Stanton number is presented. The circles, which are for natural transition, show that turbulent flow occurs approximately at a Reynolds number of 3.5×10^6. When roughness is placed on this model, the beginning of turbulent flow moves from a Reynolds number of approximately 3.5×10^6 to less than 0.7×10^6.

The model used to detect spanwise distortions (fig. 3) had three chordwise rows of thermocouples placed at different spanwise positions behind one roughness element. The roughness elements on the plate are actually closer together than is indicated in the figure. Typical data taken with this model are presented in figure 3. The results show that when the roughness is of proper size, in this case $k/\delta_k \approx 1.9$, spanwise distortion of the flow is very slight. The beginning of turbulent flow is reasonably close to the roughness, and the

experimental heat-transfer measurements are approximately those calculated by the Spalding-Chi method (ref. 9) when the virtual origin is assumed to be located at the trip. However, if k/δ_k is decreased to approximately 1.4, the spanwise variation behind the roughness element is considerably increased. The flow becomes uniform spanwise at approximately 8 inches from the leading edge. This position would be chosen as the beginning of turbulent flow and is the position identified as the virtual origin for the calculation shown. However, if the roughness is made too high, spanwise distortions appear for the entire length of the instrumentation as can be seen when $k/\delta_k \approx 5.4$. The trends of the data for this condition are no longer similar to those calculated for turbulent flow. These data are taken at conditions where the spanwise distortions can be minimized by properly sizing the trips. At higher Mach numbers, where the maximum Reynolds number of wind-tunnel facilities is limited, spanwise distortions may always exist.

Roughness-Transition Parameters

The more important roughness-transition parameters are as follows:

(1) Pressure gradient
(2) Wall temperature
(3) Spacing
(4) Local Mach number
(5) Roughness-position Reynolds number $R_{x,k}$
(6) Unit Reynolds number
(7) Type of roughness
(8) Roughness-height Reynolds number R_k
(9) Model configuration

The pressure gradient and wall temperature are not included in the present discussion. In reference 5 the spacing of the roughness elements was not found to be critical at supersonic Mach numbers. (However, these elements should not be too closely spaced.) Similar trends have been noted at Mach 6. In this investigation the lateral spacing between the elements has generally been made 4 times the width of the element (or larger).

In figure 4, the effect of varying the last three parameters in the foregoing list while the other parameters are kept unchanged is examined. Bear in mind that the object is to find the most effective trip that has the smallest drag. The effect of using various types of roughness to trip the boundary layer on a flat plate is shown on the left side of figure 4, where the transition Reynolds number is plotted against the height of the roughness. The various types of roughness elements are indicated in the figure. The type of roughness element is not too important in producing transition; however, apparently an appreciable part of the area of the element must be located near the top. For example the data show that the pyramidal roughness does not trip the flow as well as the other types. On the other hand, a pinhead type of roughness which has its largest area near the top seems to be as good as (or better than) any trip tried. The pinhead is of interest as it would reduce the frontal area of the trip and thus probably reduce the pressure drag associated with the

trip. However, the drag reduction is limited in that the area decrease takes place on that portion of the element which experiences the lowest pressures; furthermore, there is a strong possibility that the flow below the head of the pin would become choked, whereby some of the possible benefits would be negated.

On the right-hand side of figure 4 the effects of tripping the boundary layer on a delta wing and a flat plate are compared. The results indicate that the flow on a delta wing is easier to trip than that on a flat plate.

The effect of the roughness-position Reynolds number $R_{x,k}$ is now examined. This Reynolds number is based on conditions at the edge of the boundary layer and the distance from the leading edge to the roughness position. Another Reynolds number must be defined for this discussion. This Reynolds number $R_{k,c}$ is the Reynolds number based on conditions at the top of the roughness element necessary to move turbulent flow close to the trip position. (Turbulent flow is probably never moved completely to the roughness position.) Most previous data were taken at positions where $k/\delta_k < 1$ and have shown that the Reynolds number necessary to move turbulent flow close to the trip, $R_{k,c}$, is not a function of the roughness-position Reynolds number, $R_{x,k}$, if $R_{x,k} > 10^5$ (ref. 1). However, the present data show that at a Mach number of 6, $R_{k,c}$ is a function of the roughness-position Reynolds number $R_{x,k}$. It is true that k/δ_k must be greater than 1 for the Mach 6 data, whereas previously most of the available data were taken under conditions where $k/\delta_k < 1$. This difference in k/δ_k may explain why $R_{k,c}$ is a function of $R_{x,k}$. However, the important point is that when $k/\delta_k > 1$, a plot of the Reynolds number necessary to move transition close to the roughness position must consider $R_{x,k}$. At a Mach number of 6, $R_{x,k}$ has been varied by a factor of 10, and the values of $R_{k,c}$ for these conditions are shown in figure 5. This figure includes other data obtained on a flat plate or a cone. The data shown for $M_l < 4$ and $k/\delta_k < 1$ are from reference 10 which includes other sources. Also included are some data at supersonic conditions which have been taken at the Ames Research Center for $k/\delta_k > 1$. However, not enough data are available to determine the effect of $R_{x,k}$ for the Ames Center data.

Although data at Mach numbers greater than 6 are very limited, indications are that the values of R_k required to move turbulent flow close to the roughness position become very large and increase rapidly above approximately Mach 6. This result is indicated by the correlation of Potter and Whitfield* from reference 11 which is plotted in figure 5 and also by some unpublished data taken on a flat plate at a local Mach number of 8 by P. Calvin Stainback at the Langley Research Center. Stainback's roughness had a value of R_k approximately equal to 1.7×10^4 $\left(R_{x,k} \approx 0.19 \times 10^6\right)$ but the position of transition was not decreased at all. On the other hand, McCauley (ref. 12) presents data

*The correlation of Potter and Whitfield given in reference 11 is in a different form than that presented in figure 5.

at a local Mach number of approximately 8.5 where $R_k \approx 1.5 \times 10^4$ $\left(R_{x,k} \approx 10^6\right)$ and the transition Reynolds number was decreased by a factor of approximately 2. (Note that the $R_{x,k}$ value of McCauley's data was larger than that for Stainback's data.) The main point to be noted is that at high Mach numbers, if turbulent flow can be moved to the roughness position at all, very high roughness elements must be used. However, the boundary-layer transition position can be moved forward by using smaller trips.

It should be emphasized that if $R_{x,k}$ is below some limiting value, it is extremely difficult to trip the boundary layer. (See, for example, ref. 1.) Therefore, it is not sufficient to speak of a transition parameter in terms of only boundary-layer thickness. Another way of saying the same thing is to note that if the trips are too close to the leading edge, the boundary layer may not become turbulent, even for relatively large values of k/δ_k. More information about the relationship between $R_{x,k}$ and $R_{k,c}$ when $k/\delta_k > 1$ would be helpful. This information might also be useful in predicting when spanwise distortions might be expected.

Pressure Drag of Roughness Trips

The model chosen to study the pressure drag of the trips was the wing-body configuration shown in figure 6. Sixty-nine cylindrical rods were placed on one side of the model as indicated by the figure. The drag coefficient C_D for the model with and without roughness elements as obtained from force tests is shown in figure 6. The difference between the drag coefficient for the models shown in figure 6 is due to the roughness elements. This difference can be divided into two parts: the additional skin friction due to the forward movement of transition caused by the roughness elements and the pressure drag associated with the tripping elements. The additional skin friction C_F is shown in figure 6 and was calculated by the Spalding-Chi method (ref. 9). The position of transition was determined from heat-transfer measurements on this model. The remaining C_D difference for the model with and without roughness is assumed to be the pressure drag of the elements. (This model is believed to have a detached shock and the element drag might be different for a model with an attached shock.)

On an actual wind-tunnel model, roughness trips would probably be placed on both sides of the model instead of on only one side as was done in this case. Therefore, the pressure drag associated with the roughness elements alone, for this body with trips on both sides would be approximately twice that shown in figure 6 and would be approximately 15 percent of the total drag of the body. The trip drag for a typical supersonic transport wind-tunnel model was generally less than 5 percent of the total (ref. 1).

The methods applied at supersonic speeds to determine roughness element drag (ref. 1) seem to be no longer applicable at hypersonic conditions. Work is presently being conducted in an attempt to determine experimentally the trip

drag directly at hypersonic speeds. At this time, however, trips cannot be used when an accurate value of the total drag of a configuration is required.

The size of the roughness necessary to move transition close to the trips for the higher Mach numbers becomes very large, as is indicated by the over-simplified results shown in figure 7. The large sizes can create very large spanwise effects in the boundary layer in addition to the large pressure drag ΔC_D associated with the trip elements. For this reason, at high Mach numbers, tripping of the flow will probably be limited to those conditions where the transition distance from the leading edge is decreased to approximately 1/2 or 1/4 of that occurring with natural transition.

It also desirable to decrease the pressure drag of the trips. One method suggested is to decrease the frontal area of the roughness element by using a pinhead type of roughness. The limitations of this method have been previously discussed. One promising method of minimizing the drag of the element is to use air jets as tripping elements, since it is difficult to transmit the force associated with the column of air to the model, but some inherent disadvantages are associated with using an air jet in model testing. Because this method does offer some promise, it appears to be worth further investigation. (Ref. 13 includes some examples of tripping by air jets.)

Comparison of the Heat Transfer With and Without Trips

For the purpose of investigating whether a natural turbulent boundary layer and a tripped turbulent boundary layer have the same heat transfer (and skin friction), measurements were made on a flat plate and a 20° wedge both with and without trips. The model is shown at the top of figure 8. The Reynolds number on the wedge can be varied both by moving the position of the wedge and by placing trips on the model. The results are given in figure 8 where the Stanton number is plotted against Reynolds number R_V (based on the distance from the virtual origin). Thus, the data can be compared on an equivalent Reynolds number basis. The virtual origin is taken as the experimentally determined beginning of turbulent flow. The data for both the smooth and the rough plate are approximately the same both on the plate and on the wedge. This comparison seems to indicate that if roughness of the proper size is used, a tripped turbulent boundary layer gives the same heat transfer as a natural turbulent boundary layer. One difference is indicated, however, by the oil patterns shown in figure 9 which were obtained on the same plate but with a 40° wedge. The position of the roughness elements and the wedge are indicated in the figure. Initially dots of oil were placed on this plate. Downstream of the roughness elements on the plate, no influence of the roughness elements is indicated except close to the elements; whereas, on the wedge there is a trace or a wake directly behind each of the roughness spheres. In order to determine the effect of these wakes, thermocouples were placed on the wedge as is indicated by the arrows. Only small spanwise differences in the heating rates along these various rows were found, and the wakes are consequently considered to be only a secondary influence that can be ignored as a design factor for most engineering studies. (These spanwise differences, however, might be important in fluid-mechanics

studies.) From these data, a tripped turbulent boundary layer is concluded to have the same heat transfer as a natural turbulent boundary layer if the roughness elements are of proper size.

Roughness on Delta Wings

Oil-flow studies on a delta wing with a natural turbulent boundary layer and separation are now examined. The delta wing with a trailing-edge flap is shown in figure 10. Also shown in the figure is the approximate position of the beginning of fully turbulent flow as determined by heat-transfer methods. Previous studies have shown that whether separation occurs depends strongly upon whether the flow is laminar, transitional, or turbulent (e.g., refs. 14, 15, and 16). This result is also found in the present studies. For example, it is observed in figure 10 that when the flap is at 30°, separation occurs along the edges of the model where transitional or laminar flow exists, whereas on the center of the wing where the flow is turbulent, the flow does not separate. When the flap angle is increased to 40°, separation occurs in front of the entire flap on the wing. This flow is very complex, and the oil patterns show that there are several vortices existing on the surface of the plate. The sketch in figure 10 indicates a simplified flow model constructed from a study of the oil patterns. Apparently, there is a vortex flow lifting off the surface in the separation region and reattaching onto the flap. It is believed that the vortex pattern results from the fact that at the chordwise location of the vortex, the flow is turbulent on the center of the wing and is transitional or laminar near the edge of the wing. The difference in the surface shear forces produces the vortex flow pattern, which is a different type of transitional separation than that observed in two-dimensional flow.

Examples of the effects of placing roughness elements near the leading edges of the wing are shown in figure 11. With the roughness elements on the wing an entirely different type of separated flow occurs than was previously observed without roughness. The explanation for this difference appears to be that the roughness trips the boundary layer ahead of the wing-flap junction and thereby provides a turbulent spanwise flow prior to separation. Supporting this conclusion is figure 11(c) in which the same configuration is placed at a 5° angle of attack. In this case, the local Reynolds number is increased and a spanwise turbulent boundary layer develops naturally prior to separation, so that a flow similar to that of figure 11(b) is produced.

A certain amount of outflow from the separated region occurs in the vicinity of the wing-flap juncture. This phenomenon indicates one of the problems of using roughness elements in separated flow for delta-wing configurations. For example, the roughness elements close to the edge of the wing in the separated region would probably change the amount of outflow from the value that would be obtained with natural turbulent-boundary-layer conditions. Figure 11 also suggests that difficulty would be encountered in making tip-control studies when turbulent flow is produced by trips, inasmuch as at least a short run of turbulent flow behind a trip is desirable before the flow encounters a control surface. It is concluded that trips can be useful in wind-tunnel tests of

delta wings if consideration is given to the local flow and the purpose of any particular investigation.

The two oil-flow photographs of the model at $\alpha = 0^{\circ}$ in figure 11 show a major difference in the flow patterns that develop for the turbulent separated condition (with roughness) when compared with the transitionally separated condition (no roughness). Although the data are not shown, the pressure and heat transfer for these two conditions show that forward of the flap junction, only minor variations occur. Over the flap portion of the transitionally separated model, a loss occurs in the integrated pressure level as compared with that of the model with roughness, with its more nearly two-dimensional separation. A comparison of the experimental data with the two-dimensional calculations presented in reference 15 shows that present prediction methods are useful in predicting pressure and heat-transfer magnitudes for delta wings with complete turbulent separated flow ahead of the flap-wing junction. However, more work is required on delta-wing configurations with transitional separation.

In figures 12 and 13 some results obtained on this wing at an angle of attack are given. The oil patterns show that the flow is again very complex. The flow is apparently attached to the surface near the leading edge of the wing but then separates and produces a vortex flow as indicated in the sketch of figure 13. (See ref. 17 for a somewhat similar type of vortex flow.) The vortex flow reattaches near the center line and then apparently reseparates to produce the feather like appearance shown in figure 12. This is a rather shallow type of separated flow, as can be seen by inspecting the oil flows with the flap at 30°, where the flow reattaches to the surface very close to the flap-wing junction. The pressure distributions of figure 13 also indicate this shallow type of separation. Another point to be noted is that the flow for these conditions is apparently very difficult to trip, and simulation of naturally turbulent conditions may be impossible. Both pressure and heat-transfer measurements have been made with various sizes of roughness elements near the leading edge. It has not been determined whether this flow was made turbulent by the use of trips. However, it appears to be extremely difficult, if not impossible, to obtain a simulation of flight behavior in a wind tunnel by using trips under conditions where the behavior on the lee side shown in figure 12 occurs. (Ref. 18 gives a more detailed discussion of this problem at supersonic speeds.) On the other hand, it may not be necessary to duplicate Reynolds number conditions with vortex shedding near the leading edge. (Nevertheless, it should be mentioned that research at lower Mach numbers (ref. 18) indicates that the Reynolds number does affect the flow associated with vortices.) This phenomenon needs additional study since hypersonic-cruise vehicles will probably encounter flow fields similar to this.

CONCLUDING REMARKS

Boundary layers have been made turbulent by roughness elements up to local Mach numbers of approximately 9 or higher. However, the size of the roughness necessary to move transition close to the trips for the higher Mach numbers becomes very large. The large size of the trips can create very large spanwise effects in the boundary layer and large pressure drags associated with the trip

elements. For this reason, at high Mach numbers tripping will probably be limited to those conditions where the transition distance from the leading edge will be decreased to approximately 1/2 or 1/4 of that occurring with natural transition.

Whether roughness should be used to promote turbulent flow in hypersonic wind-tunnel tests depends upon the particular purpose of any experiment. For example, trips can be used successfully to study the heat transfer associated with an aircraft component or to produce turbulent flow in front of an inlet or control that might otherwise be transitional or laminar. However, at the present time, trips cannot be used when an accurate value of the total drag of a configuration is required because of the large pressure drag associated with the roughness elements. Additional work is necessary to determine the pressure drag of the elements with reasonable accuracy. Another problem for study is the use of trips for wind-tunnel simulations of hypersonic-cruise vehicles when vortex shedding occurs on the lee side of delta wings at moderate angles of attack. For any test, care must be taken to provide roughness elements of proper size.

REFERENCES

1. Braslow, Albert L.; Hicks, Raymond M.; and Harris, Roy V., Jr.: Use of Grit-Type Boundary-Layer-Transition Trips on Wind-Tunnel Models. Conference on Aircraft Aerodynamics, NASA SP-124, 1966, pp. 19-36. (Also, available as NASA TN D-3579.)

2. Holloway, Paul F.; and Sterrett, James R.: Effect of Controlled Surface Roughness on Boundary-Layer Transition and Heat Transfer at Mach Number of 4.8 and 6.0. NASA TN D-2054, 1964.

3. Stainback, P. Calvin: Some Effects of Roughness and Variable Entropy on Transition at a Mach Number of 8. AIAA Paper No. 67-132, Jan. 1967.

4. Korkegi, Robert H.: Transition Studies and Skin-Friction Measurement on an Insulated Flat Plate at a Mach Number of 5.8. J. Aeron. Sci., vol. 23, no. 2, Feb. 1956, pp. 97-107, 192.

5. Van Driest, E. R.; and McCauley, W. D.: The Effect of Controlled Three-Dimensional Roughness on Boundary-Layer Transition at Supersonic Speeds. J. Aero/Space Sci., vol. 27, no. 4, Apr. 1960, pp. 261-271, 303.

6. Fay, J. A.; and Goldburg, A.: Vortex Shedding, Transition and Growth of Luminous Wakes Behind Spheres at Mach 15 to 25. Res. Note 295(BSD-TDR-62-105), Avco-Everett Res. Lab., Apr. 1962.

7. Hall, Gordon R.: Interaction of the Wake From Bluff Bodies With an Initially Laminar Boundary Layer. AIAA Paper No. 66-126, Jan. 1966.

8. Potter, J. Leith; and Whitfield, Jack D.: Effects of Unit Reynolds Number, Nose Bluntness, and Roughness on Boundary Layer Transition. AEDC-TR-60-5, U.S. Air Force, Mar. 1960.

9. Spalding, D. B.; and Chi, S. W.: The Drag of a Compressible Turbulent Boundary Layer on a Smooth Flat Plate With and Without Heat Transfer. J. Fluid Mech., vol. 18, pt. 1, Jan. 1964, pp. 117-143.

10. Braslow, Albert L.: Review of the Effect of Disturbed Surface Roughness on Boundary-Layer Transition. AGARD Rept. 254, Apr. 1960.

11. Potter, J. Leith; and Whitfield, Jack D.: Boundary-Layer Transition Under Hypersonic Conditions. Recent Developments in Boundary Layer Research, Pt. III, AGARDograph 97, May 1965, pp. 1-62.

12. McCauley, W. D.; Saydah, A.; and Bueche, J.: The Effect of Controlled Three Dimensional Roughness on Hypersonic Laminar Boundary Layer Transition. AIAA Paper No. 66-26, Jan. 1966.

13. Nagel, A. L.; Savage, R. T.; and Wanner, R. (With appendix by R. W. Blank): Investigation of Boundary Layer Transition in Hypersonic Flow at Angle of Attack. AFFDL-TR-66-122, U.S. Air Force, Aug. 1966. (Available from DDC as AD 803 781.)

14. Chapman, Dean R.; Kuehn, Donald M.; and Larson, Howard K.: Investigation of Separated Flows in Supersonic and Subsonic Streams With Emphasis on the Effect of Transition. NACA Rept. 1356, 1958. (Supersedes NACA TN 3869.)

15. Holloway, Paul F.; Sterrett, James R.; and Creekmore, Helen S.: An Investigation of Heat Transfer Within Regions of Separated Flow at a Mach Number of 6.0. NASA TN D-3074, 1965.

16. Arrington, James P.; Molloy, John K.; and Goldberg, Theodore J.: Flare-Stabilization Problems at Hypersonic Mach Numbers. AIAA Sounding Rocket Vehicle Technology Specialist Conference, Feb.-Mar. 1967, pp. 84-91.

17. Rainbird, W. J.; Crabbe, R. S.; Peake, D. J.; and Meyer, R. F.: Some Examples of Separation in Three-Dimensional Flows. Quart. Bull. No. 1, Div. Mech. Eng. & Natl. Aeron. Estab., Natl. Res. Council Can., 1966, pp. 1-52.

18. Rein, J. A.: Flow Over the Suction Surface of Sharp Edge Delta Wings With Detached Leading Edge Shock Waves. Tech. Note HSA 102, Weapons Res. Estab., Australian Defence Sci. Serv., Dec. 1964.

PAINT PATTERN DOWNSTREAM OF ROUGHNESS ELEMENT

5° BLUNTED CONE; $M_\infty \approx 8$; $k/\delta_k \approx 2.4$

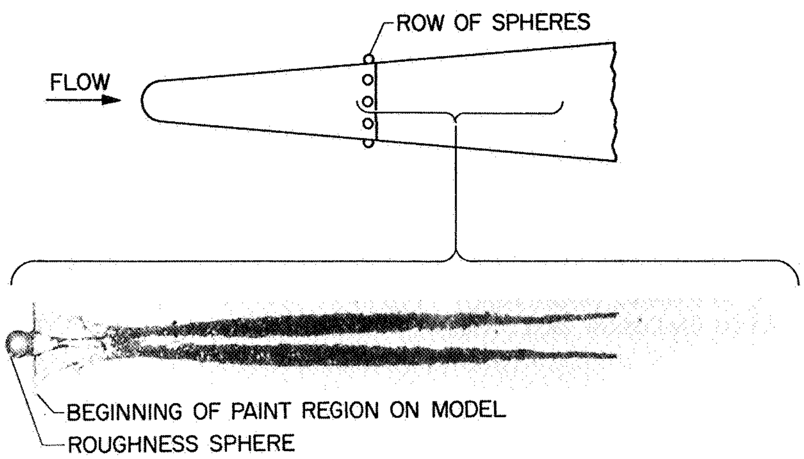

Figure 1 L-2865-10

METHODS FOR DETECTING TRANSITION

FLAT PLATE; $M_\infty = 6$

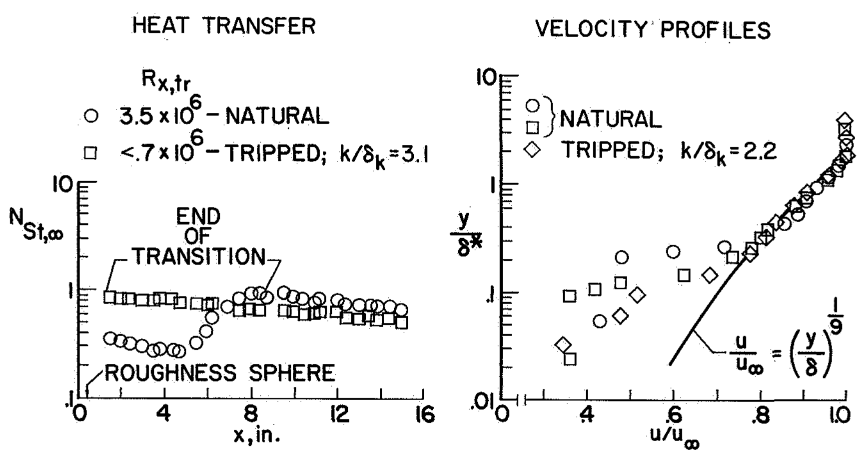

Figure 2

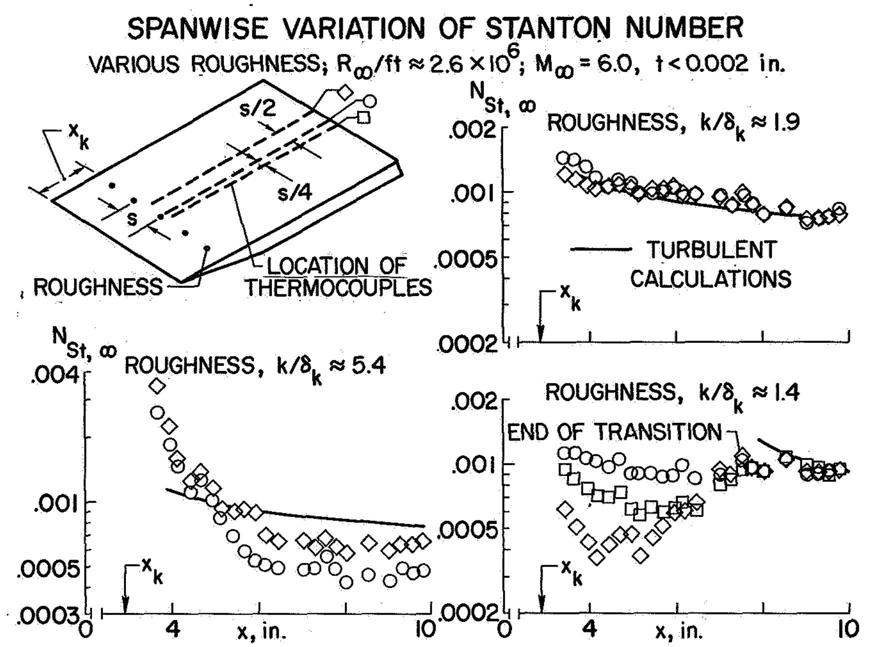

Figure 3

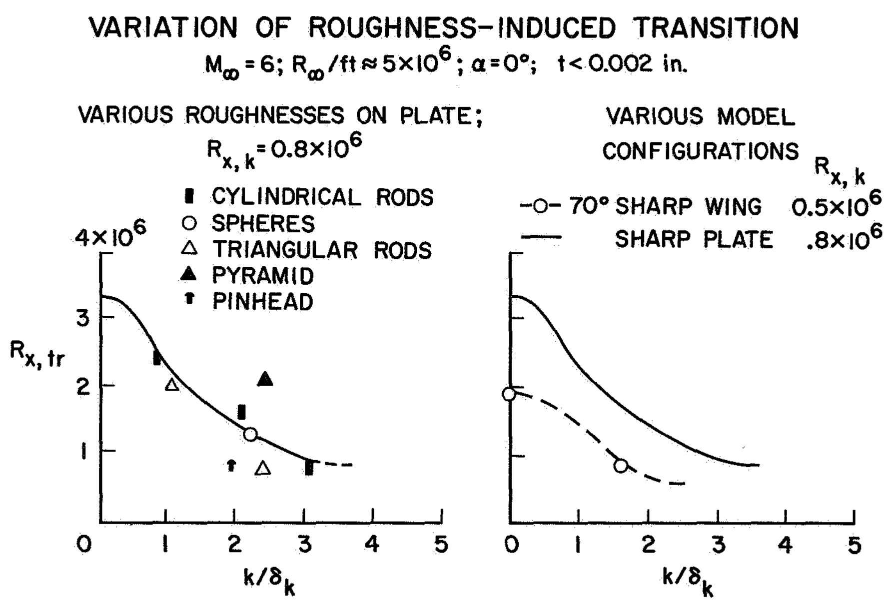

Figure 4

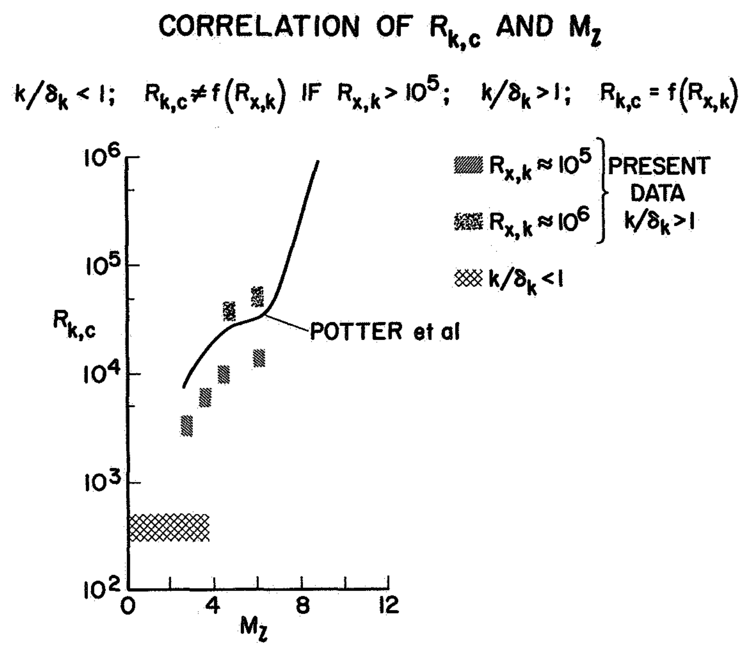

Figure 5

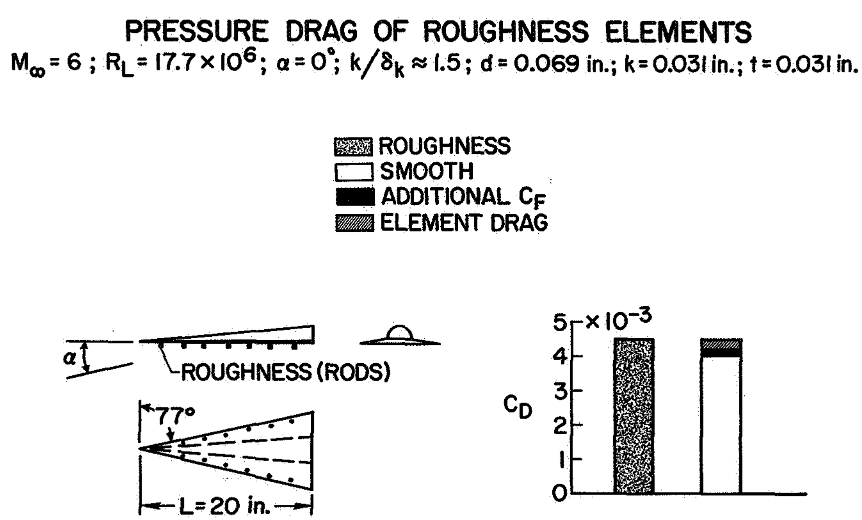

Figure 6

TRANSITION CLOSE TO ROUGHNESS

TYPICAL TUNNEL CONDITIONS FOR A PLATE

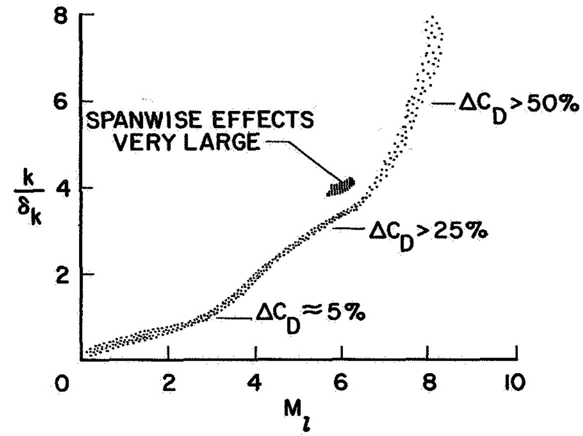

Figure 7

HEAT TRANSFER WITH AND WITHOUT ROUGHNESS

$M_\infty = 6$; $R_\infty/\text{ft} \approx 8.0 \times 10^6$; $t < 0.002$ in.; $s = 0.31$ in.; $\delta_f = -20°$

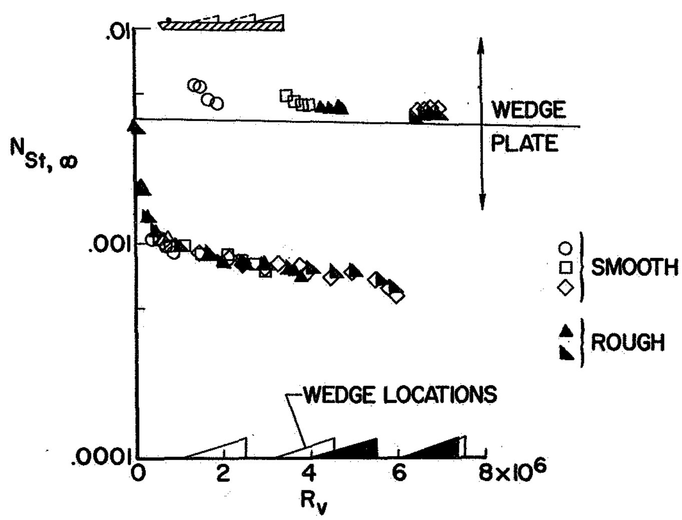

Figure 8

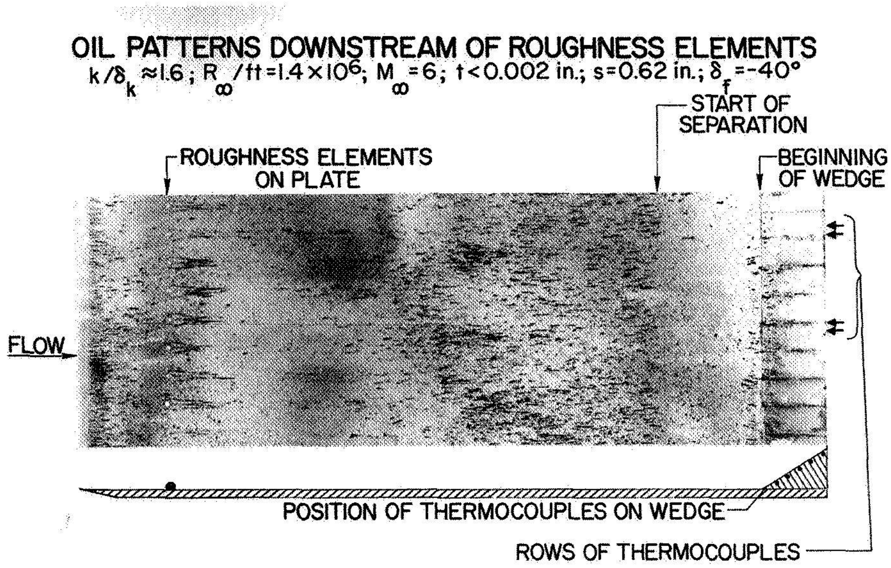

Figure 9 L-2865-3

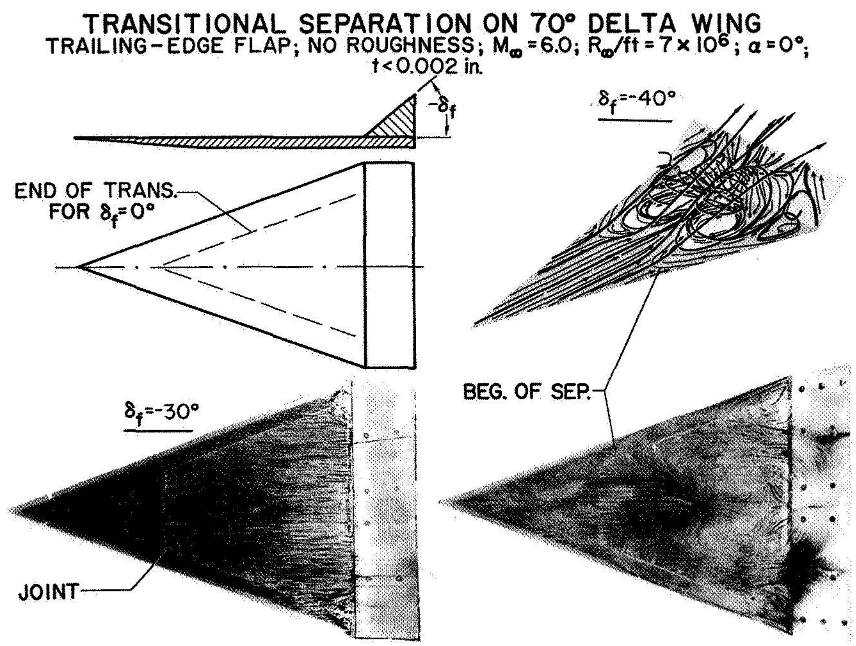

Figure 10 L-2865-6

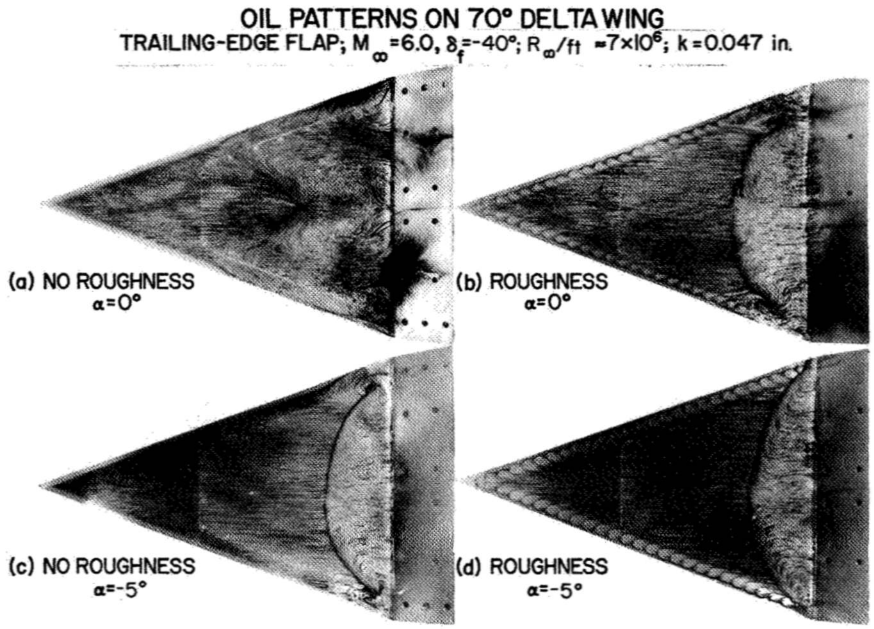

Figure 11 L-2865-1

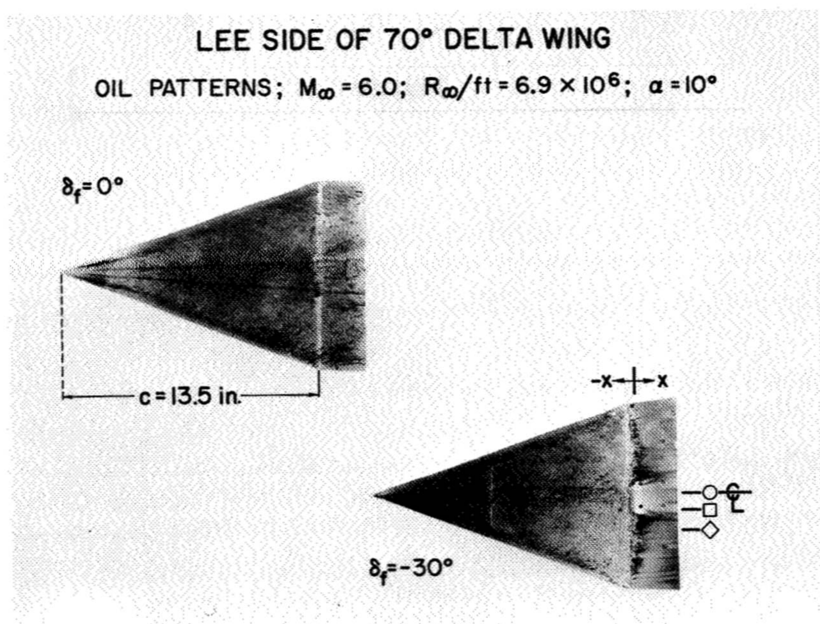

Figure 12 L-2865-11

LEE SIDE OF 70° DELTA WING

$M_\infty = 6.0$; $R_\infty/ft = 6.9 \times 10^6$; $\alpha = 10°$

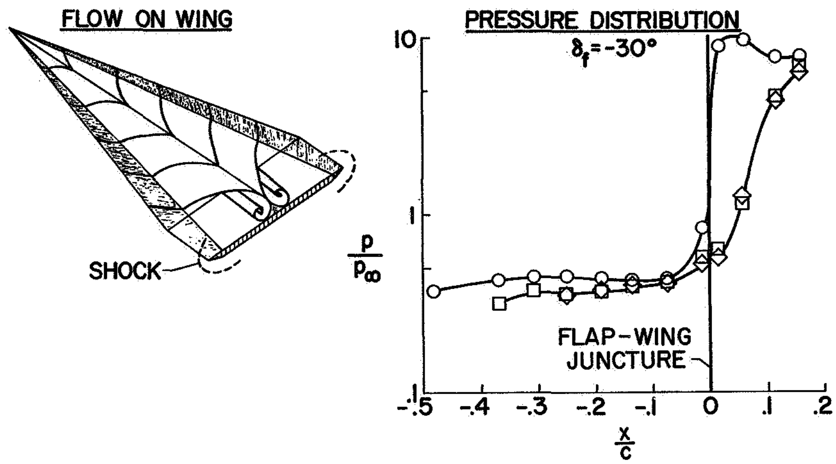

Figure 13